האגוד הישראלי למכניקה עיונית ושימושית

The Israel Society for Theoretical and Applied Mechanics

ISTAM

An Adhering Organization of the
International Union of Theoretical and Applied Mechanics
(IUTAM: http://www.iutam.net**)**

ISTAM Annual Symposium

TECHNICAL PROGRAM

5 December 2010

Tel Aviv University

ISTAM Annual Symposium

5 December 2010

TECHNICAL PROGRAM

Location: Rosenblatt Auditorium, Computer and Software Engineering Building, Tel Aviv University

09:30 – 09:50 Registration and coffee

09:50 – 10:00 *Opening:* MB Rubin, Technion

Morning Session Chairman: MB Rubin, Technion

K Wilmanski Technical University, Berlin. *Permeability, tortuosity and attenuation of waves in porous materials* 10:00 – 10:45

10:45 – 11:15 **L Heller**, L Banks-Sills, V Fourmann. Tel Aviv University. *A fracture criterion for cracks parallel to the poling direction of piezoelectric PZT-5H ceramics*

11:15 – 11:45 **EH Rejovitzky**, Technion. *Non-commutative damage accumulation due to material heterogeneity*

11:45 – 12:15 **G Moiseyev**, S Givli, PZ Bar-Yoseph. *Building 'bottom-up' Blood Coagulation models using Statistical Mechanics*

12:15 – 12:30 ISTAM Business meeting - Approval of Prof. Zohar Yosibash from Ben Gurion University as ISTAM's second representative to the General Assembly of IUTAM

12:30 – 14:00 Lunch (The registration fee includes lunch)

Afternoon Session Chairman: T Miloh, Tel Aviv University

In Memory of Prof. Isaac Goldhirsch

14:00 – 14:30 **G Dagan**, Tel Aviv University. *Effective conductivity of an ensemble of porous spheres*

14:30 – 15:00 **D Weihs**, Technion. *Artificial nano-flyers and nano-swimmers moving in Stokes flow*

G Ben-Dor, Ben Gurion University. *Hysteresis phenomena in the interaction of shock waves in steady flows* 15:00 – 15:30

V Steinberg, Weizmann. *Single vesicle dynamics in various flows: Experiment versus theory* 15:30 – 16:00

SH Noskowicz, Tel Aviv University. *Granular gases and kinetic theory* 16:00 – 16:30

The annual membership fee to ISTAM is 100 NIS. It includes the lunch at the symposium and can be paid during the registration.

All lectures are open to the public free of charge

Permeability, tortuosity, and attenuation of waves in porous materials

Krzysztof Wilmanski

TU (Berlin) and ROSE School (Pavia)
Email: wilmansk@wias-berlin.de

The main difference in macroscopic description of composites and porous materials arises due to diffusion processes in the latter. Such processes are modeled by the so-called immiscible mixtures which admit relative motion of components. This relative motion yields in turn the irreversibility of processes as, similarly to other processes of internal friction, they dissipate energy due to the resistance of the solid component – skeleton –to the motion of fluid components. The resistance is characterized by material parameters called permeability and tortuosity. As a consequence of this dissipation acoustic waves in such materials are attenuated.

In the lecture we present fundamental properties of permeability and tortuosity in linear models of porous materials. We limit the attention to linear models as they are applied to the description of acoustic waves of small amplitude for which deviations from the initial state can be assumed to be small. For simplicity we limit considerations to two-component materials, i.e. we assume that the porous material is saturated.

In continuous models satisfying these assumptions we have to formulate field equations for the following quantities

$$\left\{\rho^S, \rho^F, n, \mathbf{v}^S, \mathbf{v}^F, \mathbf{e}^S, \theta^S, \theta^F\right\}, \tag{1}$$

where ρ^S, ρ^F are current mass densities of the skeleton and of the fluid, respectively, n denotes current porosity, $\mathbf{v}^S = v_i^S \mathbf{e}_i$, $\mathbf{v}^F = v_i^F \mathbf{e}_i$ are macroscopic (average) velocities of both components and $\mathbf{e}^S = e_{ij}^S \mathbf{e}_i \otimes \mathbf{e}_j$ is the Almansi-Hamel measure of small deformations of the skeleton, θ^S, θ^F are partial absolute temperatures of components. Obviously, $\mathbf{e}_i, i = 1,2,3, \mathbf{e}_i \cdot \mathbf{e}_j = \delta_{ij}$, denote the base vectors of the Cartesian frame of reference.

The problem of nonisothermal processes with different temperatures plays an important role in many practical applications such as transport of water in soils (e.g. by freezing processes) or transpiration cooling in aerospace engineering. However, its thermodynamic foundations are not clear as yet and we shall not consider them it in this lecture.

Governing equations for the fields (1) with constant temperatures $\theta^S = \theta^F = \theta = const.$ follow from partial balance equations of mass and momentum.. They have the form

$$\begin{gathered} \frac{\partial \rho^S}{\partial t} + \rho_0^S \operatorname{div} \mathbf{v}^S = 0, \quad \frac{\partial \rho^F}{\partial t} + \rho_0^F \operatorname{div} \mathbf{v}^F = 0, \\ \rho_0^S \frac{\partial \mathbf{v}^S}{\partial t} = \operatorname{div} \mathbf{T}^S + \hat{\mathbf{p}}^S + \rho_0^S \mathbf{b}^S, \quad \rho_0^F \frac{\partial \mathbf{v}^F}{\partial t} = \operatorname{div} \mathbf{T}^F + \hat{\mathbf{p}}^F + \rho_0^F \mathbf{b}^F, \end{gathered} \tag{2}$$

while the balance equation of porosity is as follows

$$\frac{\partial \Delta_n}{\partial t} + \Phi_0 \operatorname{div}\left(\mathbf{v}^F - \mathbf{v}^S\right) = \hat{n}, \quad \Delta_n = n - n_E. \tag{3}$$

We neglect mass sources and nonlinear kinematical contributions. $\mathbf{T}^S = \sigma_{ij}^S \mathbf{e}_i \otimes \mathbf{e}_j, \mathbf{T}^F = \sigma_{ij}^F \mathbf{e}_i \otimes \mathbf{e}_j$ denote partial stress tensors. As we assume the fluid component to be inviscid on the macroscopical level we have

$$\mathbf{T}^F = -p^F \mathbf{1} \quad \text{i.e.} \quad \sigma^{\mathrm{F}}_{\mathrm{kk}} = -3p^F, \tag{4}$$

where p^F is the partial pressure in the fluid. $\hat{\mathbf{p}}^S, \hat{\mathbf{p}}^F$ are momentum sources and they satisfy the momentum conservation law

$$\hat{\mathbf{p}}^S = -\hat{\mathbf{p}}^F. \tag{5}$$

$\mathbf{b}^S, \mathbf{b}^F$ are the densities of partial body forces. They may include contributions following from a noninertial frame of reference, such as centrifugal, Coriolis and Euler forces. The quantity n_E, appearing in the porosity balance equation is the so-called equilibrium porosity and $\hat{n}$ is the source of porosity. In equation (3), Φ_0 is a material constant defining the flux of porosity for isotropic materials. In the case of anisotropic materials, it would be a tensor of the second rank, $\mathbf{\Phi}_0 = \Phi_{ij}\mathbf{e}_i \otimes \mathbf{e}_j$, but we shall not discuss this kind of materials. Porosity source $\hat{n}$ may follow from damage processes of the skeleton, relaxation processes in biological tissues, etc.

In addition to balance equations, the deformation tensor of the skeleton must satisfy the usual integrability condition of the continuum which in the linear theory has the following form

$$\frac{\partial \mathbf{e}^S}{\partial t} = \operatorname{sym}\operatorname{grad} \mathbf{v}^S \quad \Rightarrow \quad \frac{\partial e}{\partial t} = \operatorname{div} \mathbf{v}^S. \tag{6}$$

The second equation describes volume changes of the skeleton, e.

For poroelastic materials the second law of thermodynamics yields fairly explicit constitutive relations which are needed for the following quantities

$$\left\{\mathbf{T}^S, p^F, \hat{\mathbf{p}}^S, n_E, \hat{n}\right\}. \tag{7}$$

For isotropic materials they have the following

$$\begin{aligned} \mathbf{T}^S &= \mathbf{T}_0^S + \lambda^S e\mathbf{1} + 2\mu^S \mathbf{e}^S + Q\varepsilon\mathbf{1} + \underline{\beta(n - n_E)}\mathbf{1} - N(n - n_0)\mathbf{1}, \\ p^F &= p_0^F - Qe - \rho_0^F \kappa\varepsilon + \underline{\beta(n - n_E)} + N(n - n_0), \\ \hat{\mathbf{p}}^S &= -\hat{\mathbf{p}}^F = \pi(\mathbf{v}^F - \mathbf{v}^S), \quad n_E = n_0(1 + \delta e), \quad \varepsilon = \frac{\rho_0^F - \rho^F}{\rho_0^F}. \end{aligned} \tag{8}$$

Obviously, material parameters $\lambda^S, \mu^S, \kappa, Q, N, \beta$ describe elastic properties of components, their interactions through volume changes and nonequilibrium deviation of porosity. However, the main topic of the lecture are the properties of the coefficient π - the permeability coefficient – in the momentum source which, obviously, describes the diffusive force. In the range of high frequencies this coefficient has hereditary properties. In order to expose better its other properties we skip this problem in this presentation. In addition, it is in many cases of practical bearing (e.g. for diffusion in human brain) a tensor second rank rather than a scalar as the medium may possess anisotropic properties for relative motions. This problem shall not be discussed in any details either. However we account for complex geometry of channels in porous materials by demonstrating a dependence of the permeability coefficient on the so-called tortuosity, τ, which for isotropic diffusion is a fraction of the length of the streamline between two points to the distance between those two points. These are measurable quantities and we demonstrate some results of corresponding NMR (nuclear magnetic resonance) experiments. One of the simple forms of the permeability coefficient which we use in the presentation follows from the classical Blake-Kozeny relation

$$\pi = \pi_0 \tau^2, \quad \pi_0 = \frac{n_0 \mu_v}{B}. \tag{9}$$

In this relation μ_v is the kinematical viscosity of the fluid and B - the so-called conductivity. The model is then used to describe properties of acoustic waves in porous media. We emphasize the influence of tortuosity on properties of these waves and, in particular, on the attenuation of these waves. We also show that claims in literature that the tortuosity effect is described by the so-called added mass effects are wrong. These enter the equations through the relative accelerations with the coefficient ρ_{12}.

For instance, a numerical analysis for the following data (approximately describing Fontainebleau sandstone)

$$\rho_0^S = 2500\left[\mathrm{kg/m}^3\right], \quad r := \frac{\rho_0^F}{\rho_0^S} = 0.1,$$

$$c_0^S = \frac{\mu^S}{\rho_0^S} = 1500\left[\mathrm{m/s}\right], \quad \pi_0 = 10^8\left[\mathrm{kg/m}^3\mathrm{s}\right],$$

$$a = 10^{-5}\left[\mathrm{m}\right], \quad \mu_v = 1.002\times 10^{-3}\left[\mathrm{kg/m}\cdot\mathrm{s}\right].$$

(10)

yields the following speeds and attenuations of the shear wave.

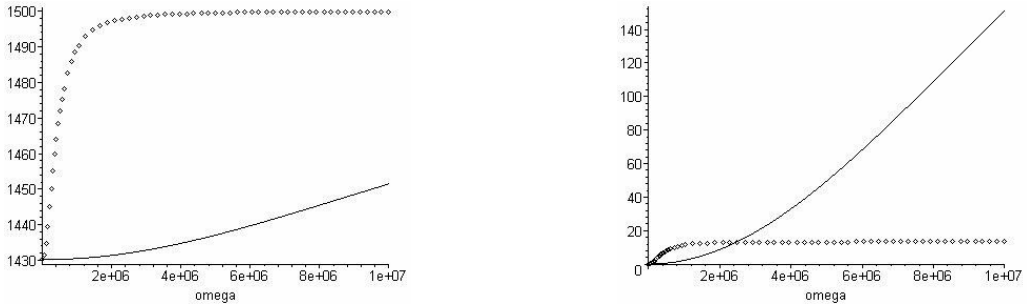

Fig. Left panel: Speed o of propagation of the shear wave c [m/s] in function of frequency ω [1/s] for the data (9) for two values of tortuosity $\tau = 1$ (dotted line) and $\tau = 6$ (solid line), **Right panel**: Attenuation of the shear wave $\mathrm{Im}k$ [1/m] in function of frequency ω [1/s] for the data (9) for two values of tortuosity $\tau = 1$ (dotted line) and $\tau = 6$ (solid line)

Changes of attenuation caused by the tortuosity yield the finite limit for $\omega \to \infty$ as required by thermodynamics. If we account for the added mass and use the so-called Berryman relation between ρ_{12} and τ then it can be easily seen that the growth of tortuosity yields the diminishing attenuation. This is, obviously, erroneous.

In conclusions we indicate some properties of surface waves which can be constructed on different boundaries of the semi-infinite porous medium.

References:

1. Wilmanski K.: *A few remarks on Biot's model and linear acoustics of poroelastic saturated materials,* Soil Dynamics & Earthquake Engineering, **26**, 6-7 (2006) 509-536.
2. Wilmanski K.: *Continuum Thermodynamics. Part I: Foundations*, New Jersey, World Scientific 2008.
3. Wilmanski K.: *Permeability, tortuosity and attenuation of waves in porous materials*, CEER, Zielona Gora, 2011 (to appear).

A fracture criterion for cracks parallel to the poling direction of piezoelectric PZT-5H ceramics

L Heller, L Banks-Sills and V Fourman

The Dreszer Fracture Mechanics Laboratory
School of Mechanical Engineering, Faculty of Engineering
Tel Aviv University, Ramat Aviv, 69970, Israel
Email: liat.hel@gmail.com

Piezoelectric ceramics are in widespread use as sensors and actuators in smart structures, despite the absence of a fundamental understanding of their fracture behavior. Piezoceramics are brittle and susceptible to cracking. As a result of the importance of the reliability of these devices, there has been tremendous interest in studying the fracture and failure behavior of such materials. To understand failure mechanisms of piezoelectric materials and maintain the stability of cracked piezoelectric structures operating in an environment of combined electromechanical loading, analysis of the mechanical and electrical behavior is a prerequisite.

In a previous study [1], an analytical, numerical and experimental investigation was carried out. The asymptotic expressions of stress, strain, electric flux density and electric fields were derived for a crack at an in-plane angle to the poling direction of the material. For a piezoelectric material, in addition to the usual three modes of fracture, there is a fourth mode associated with the electric field. Thus, K_I is the mode I stress intensity factor arising from opening deformation; K_{II} and K_{III} are associated with in-plane and out-of-plane shear deformation, respectively, and K_{IV} is the electric flux density intensity factor. The asymptotic expressions were used for determining the energy release rate and extending a conservative interaction energy or *M*-integral for calculating the intensity factors associated with piezoelectric material for energetically consistent boundary conditions on the crack faces. The energetically consistent boundary conditions consist of mechanical closing tractions and electric flux density on the crack surfaces resulting from the material or air within the crack or notch. In addition, tests were performed on four point bend PZT-5H fracture specimens with the poling direction parallel to the crack faces. The specimens were analyzed numerically by means of the finite element method. Finally, a mixed mode fracture criterion for piezoelectric ceramics was developed. This criterion is based upon the energy release rate and two phase angles, determined from the ratio between the intensity factors K_{IV} and K_I, for the first, and K_{II} and K_I, for the second. There was much scatter in the test results. This was a result of poor introduction of the notch in the specimens.

The main purpose of the present study is to validate this fracture criterion with another set of data from better test specimens. More tests have been carried out on new four point bend PZT-5H fracture specimens subjected to both mechanical and electrical loading. The specimens were analyzed numerically by means of the finite element method and *M*-integral. Additional line integrals have been added to the *M*-integral in the region near the notch tip. In Fig. 1a, a three-dimensional solid curve of the fracture criterion and the test results are presented. In this case, K_{II} is neglected. The critical energy release rate, $\mathcal{G}_c$, is plotted as a function of the phase angle, ψ. In Fig. 1b, a three-dimensional curve is presented. Here, the critical energy release rate, $\mathcal{G}_c$, is plotted as a function of the phase angles ψ and φ. The test data fits the failure curve/surface reasonably well.

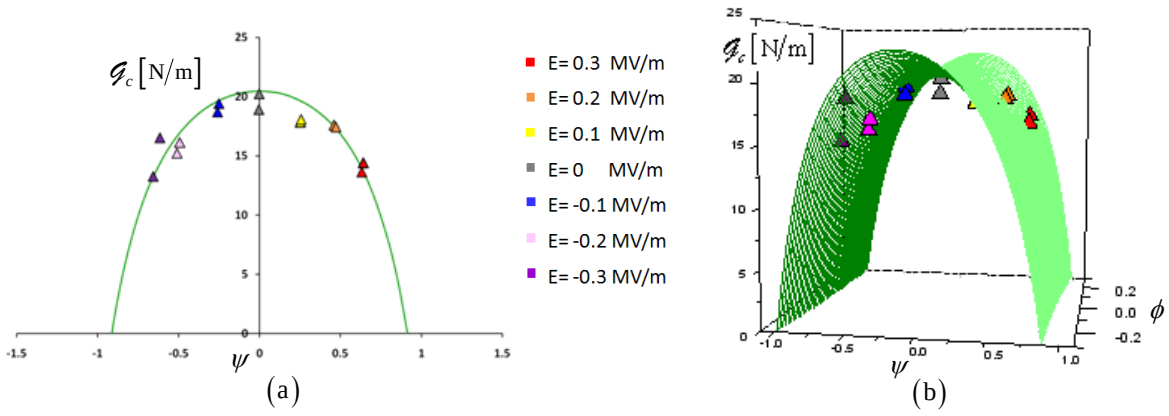

Figure 1. Fracture curve and experimental results of four-point bend PZT-5H poled specimens in (a) two dimensions and (b) three dimensions.

Reference:

Y. Motola, L. Banks-Sills and V. Fourman. On fracture testing of piezoelectric ceramics. International Journal of Fracture, 159: 167-190, 2009.

Non-commutative damage accumulation due to material heterogeneity

Elisha H. Rejovitzky[1], Eli Altus[2]

Faculty of Mechanical Engineering, Technion - Israel Institute of Technology
Haifa 32000, Israel. Email: [1]lish@tx.technion.ac.il ; [2]altus@technion.ac.il

Fatigue damage evolution includes microcrack initiation, irregular growth and stiffness degradation. A micromechanic fatigue model, which considered the above, showed macro non-commutative behaviour (High-Low vs. Low-High) which partially followed experiments. In this study, the stochastic microdamage evolution which relied on the current fatigue cycle is generalized to be dependent on the full strain history.

The material is modelled as a one dimensional set of parallel elements with stochastic damage thresholds which correspond to material defects and heterogeneity. Microcrack growth rate can be either constant or size dependent. The cycle by cycle defect accumulation is transferred to a second order non-linear differential equation of the strain evolution and analytically solved. The model is based on two material parameters. One is found from the stress-life (S-N) curve and the other is calibrated from two-level fatigue data.

Based on the above, analytical two-level fatigue envelopes are obtained. These demonstrate a non-commutative behaviour which depends on the ratio between fatigue life under the first and the second stresses ($N_{21} = N_2 / N_1$), and the threshold distribution shape only. Figure 1 presents two-level fatigue envelopes for different life ratios and threshold distribution shapes (defined by b) where N_H and N_L represent fatigue life under high and low stress-levels respectively.

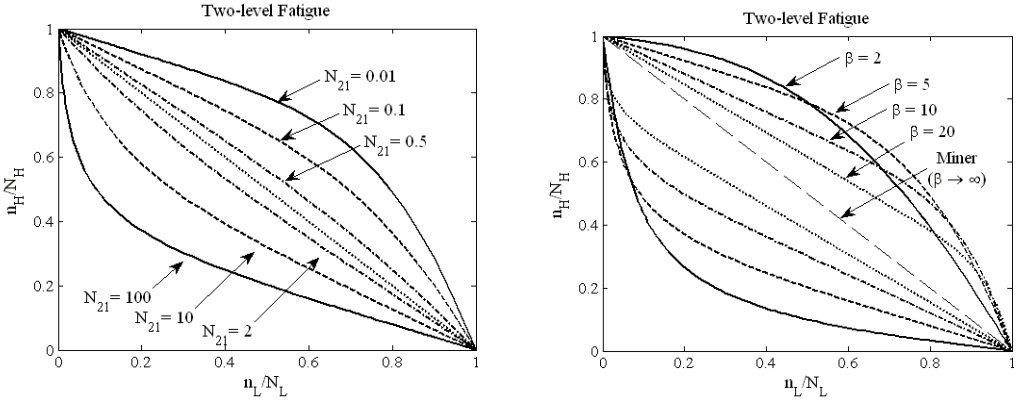

Figure 1. Two-level Fatigue Envelopes for Different Heterogeneity Levels and Stress Ratios.

In order to validate the model, an optimal value of $b = 3.45$ is determined from two-level fatigue experiments by Manson & Halford. Figure 2 shows a prediction for the whole spectrum of fatigue-life ratios.

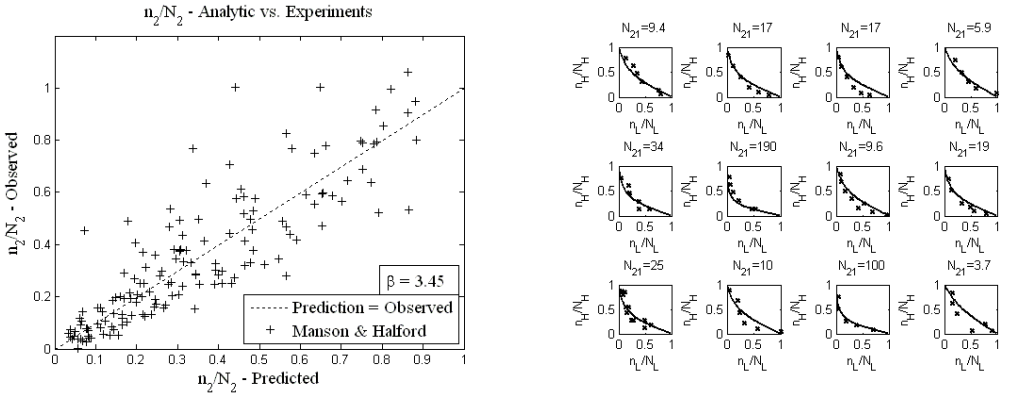

Figure 2. Two-level Fatigue – Model vs. Experiments.

Keywords: *Two-level Fatigue, Heterogeneity.*

References:

Altus, E., Nonlinear differential equation for fatigue damage evolution, using a micromechanical model. Mechanics of Materials 2002, 34:257-266.

Altus, E., Fatigue Fractals and a Modified Miner's Rule, J. App. Mech. 1991, 58:37-42.

Manson, S.S., Halford, G.R., Re-examination of cumulative fatigue damage analysis – an engineering perspective. Engineering Fracture Mechanics 1986, 25:539-571.

Building 'bottom-up' Blood Coagulation models using Statistical Mechanics

Gilead Moiseyev, Sefi Givli and Pinhas Z. Bar-Yoseph

BioMechanics Center of Excellence, Faculty of Mechanical Engineering,
Technion-Israel Institute of Technology, Haifa 32000, Israel
Email: gileadm@tx.technion.ac.il

Blood Coagulation is a complicated biological phenomenon which includes dozens of interrelated chemical reactions and activations and includes feedback loops homodynamic effects, platelet activation, interaction, and deposition. Understanding and simulating coagulation based mechanisms and pathologies are important in assessing the effectiveness, operation and safety of practically any implant that come in contact with the blood stream or placed within blood vessels, as well as blood flow related devices and procedures.

Existing models usually offer a 'top-down' point of view on blood coagulation, meaning the probability of coagulation formation or growth is derived from related macro factors, such as the vessel wall or fluid's shear stress, fluid stagnation, etc'.

The present study focuses on developing a coagulation model based on an alternative, 'bottom-up' view, in which the formation and growth of coagulated material in the blood stream will derived from behaviors of the different factors on the micro level – platelet and RBC interactions, accumulated shear induced damage in platelets, effect of the local flow regime, etc', with the 'vision' being a model which re-creates coagulation behavior from particle interactions in a manner similar to how mechanical statistics recovers the fluid's macro properties from particle interactions.

Present work has included two major mechanisms in coagulation formation and growth:

(1) Platelet activation via accumulation of damage induced by the fluid's local shear stress, for which a scheme was proposed enabling the accumulation of shear stress on any trajectory within the domain (Fig 1) and thus allowing to get a full picture of platelet flow-induced activation.

(2) Coagulation growth through polymerization of Fibrinogen monomers, for which a proposed statistical model offers a bottom-top approach, translating the interactions of coagulation polymers into forces affecting the fluid flow. The model divides the fluid into sub-domain, for which polymerization occurs on the boundaries. The proposed statistical model handles the creation/breaking of polymer bridges on the boundary (Fig 2).

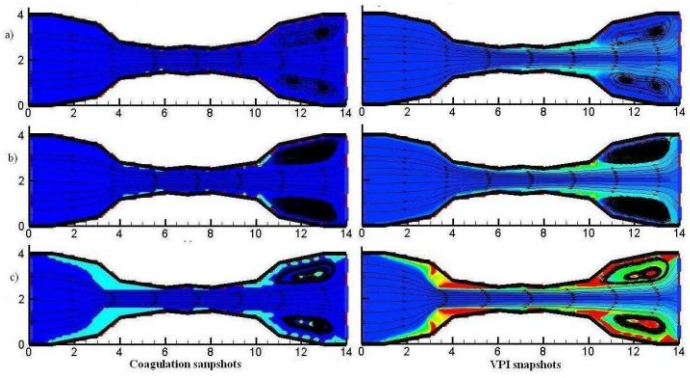

Fig 2: Schematic representation of fibrin polymerization model

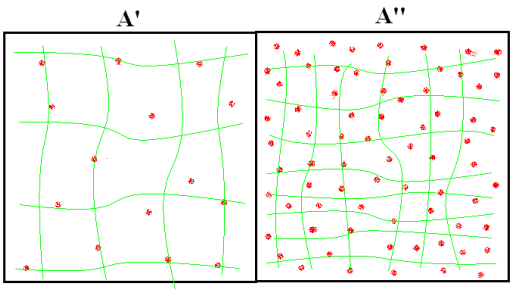

Fig 1: Coagulation model vs. accumulated shear stress scheme

Keywords: *Blood Coagulation, Mechanical Statistics.*

Reference: Moiseyev G, Bar-Yoseph PZ ,"No need for particle tracing: From accumulating fluid properties to novel blood coagulation model in the lattice Boltzmann method", Journal Of Biomechanics V43 Issue: 5 Pages: 864-870.

The following lectures are dedicated to the Memory of

Professor Isaac Goldhirsch

(1949 - 2010)

Effective conductivity of an ensemble of porous spheres

G Dagan

Faculty of Engineering,
Tel Aviv University, Israel
Email: dagan@eng.tau.ac.il

The macroscopic behaviour of granular materials was one of the major subjects investigated by Itzhak Goldhirsch. In the present lecture I am going to present some results achieved for a similar, though somewhat simpler problem. The heterogeneous medium is made up from an ensemble of a large number N of porous spheres of radius R and different permeability K_j (j=1,…N), embedded into a large sphere of radius R_0>>R, with $R/R_0 \to \infty$. The spheres are submerged in a medium of conductivity K_0, which extends to infinity. A uniform flux of magnitude U_∞ is applied at infinity. U, the mean flux in the heterogeneous medium, is equal to the space average of the local flux over the sphere of radius R_0. The effective conductivity K_{efm} of the medium is defined as the value of K_0 for which $U = U_\infty$, i.e. the presence of the heterogeneous sphere does not disturb the exterior field. This definition is equivalent to the usual one of K_{efm} as the ratio between the mean flux and the mean driving gradient. Accurate numerical solutions were obtained for a random, lognormal, distribution of K_j. The aim of the study is to demonstrate that the self-consistent approximation leads to values close to the numerical ones, for a large range of values of the volume fraction and the heterogeneity degree.

References:

I. Jankovich, A. Fiori and Dagan G., Effective conductivity of an isotropic heterogeneous medium of lognormal conductivity distribution, Multiscale Modeling and Simulations, 1(1), 40-56, 2003;.

A. Fiori, I. Jankovic and Dagan G., Effective conductivity of heterogeneous multiphase media with circular inclusions, Phys. Rev. Let., Art. No. 224502, doi: 10.1103, 94(22), June 10, 2005.

Artificial nano-flyers and nano-swimmers moving in Stokes flow

D Weihs

Head, Technion Autonomous Systems Program
Faculty of Aerospace Engineering
Technion, Haifa 32000, Israel,
Email: dweihs@tx.technion.ac.il

Design and development of a series of mm sized UAV's utilizing novel aerodynamic principles based on extremely low Reynolds number flows (Re<1)is presented.

At these sizes and Reynolds numbers, classical aerodynamics is not representative of the flow conditions, due to the dominant effects of viscosity. As a result, forces are proportional to the relative velocity,(and not squared as in high-Re aerodynamics, and any body moving in fluid drags along a large volume of fluid. The latter effect is used here to design a comb-like wing, which produces forces equal to a continuous wing at up to 90% savings in weight. These comb-like wings are similar to the wings of the insect order of Thrips, and to dandelion seeds. The theory of such combs in steady motion in Stokes flow is developed, and verified by experiment and Navier – Stokes CFD computations at low Reynolds numbers. CFD simulations of periodic flapping were performed next. Several types of models of mm-total size, and micron sized individual elements were built and tested, with results comparing very well to the theoretical predictions.

Next, we describe nano-swimmers driven by magnetic fields. The swimmers consist of a Gold body and Nickel tail each of cylindrical shape with 200 nm diameter, connected by a much thinner relatively flexible Silver wire. The total length of the swimmer is up to 6 microns. The nano-swimmers are energized by a rotating magnetic field that causes the different parts to rotate and bend producing either forward or backward motion, depending on the body parameters.

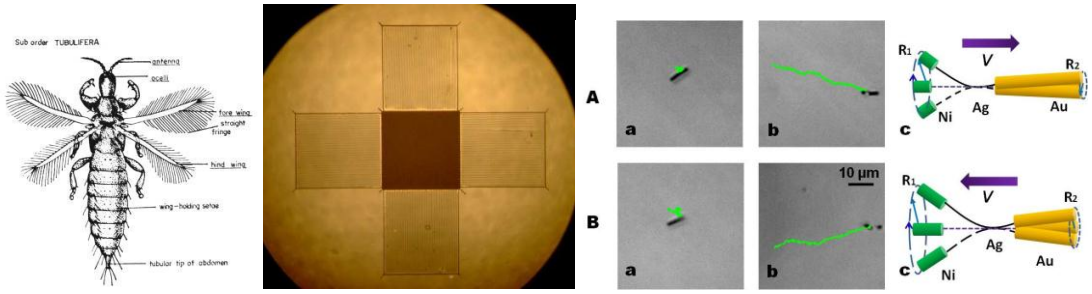

References:

E. Zussman, A.Yarin and D. Weihs, " A Micro-Aerodynamic Decelerator Based on Permeable surfaces of Nanofiber Mats", Experiments in Fluids, **33** ,315-320, 2002

E. Barta and D.Weihs: "Creeping Flow Around A Finite Row Of Slender Bodies In Close Proximity." Journal of Fluid Mechanics **551**,1-17, 2006.

D. Weihs and E. Barta,"Comb-Wings for Flapping Flight at Extremely Low Reynolds Numbers" AIAA Journal **46** (1) 285-288, 2008

W. Gao, S. Sattayasamitsathit, K. M. Manesh, D.Weihs, and J. Wang. Magnetically- Powered Flexible Metal Nanowire Motors, (submitted)

Hysteresis phenomena in the interaction of shock waves in steady flows

G Ben-Dor

Department of Mechanical Engineering
Faculty of Engineering Sciences
Ben-Gurion University of the Negev
Beer Sheva, Israel
Email: bendorg@exchange.bgu.ac.il

Ernst Mach recorded experimentally, in the late 1870s, two different shock-wave reflection configurations and laid the foundations for one of the most exciting and active research fields in an area that is generally known as *Shock Wave Reflection Phenomena*. The first wave reflection configuration, a two-shock wave configuration, is known nowadays as *regular reflection*, RR, and the second wave reflection configuration, a three-shock wave configuration, was named after Ernst Mach and is called nowadays *Mach reflection*, MR.

A monograph entitled *Shock Wave Reflection Phenomena*, which was published by Ben-Dor in 1991, summarized the state-of-the-art of the reflection phenomena of shock waves in steady, pseudo-steady and unsteady flows.

Intensive analytical, experimental and numerical investigations in the last decade, which were led mainly by Ben-Dor's research group and his collaboration with Chpoun's, Zeitoun's and Ivanov's research groups, shattered the state-of-the-knowledge for the case of steady flows. Skews's and Hornung's research groups joined in later and also contributed to the establishment of the new state-of-the-knowledge of the reflection of shock waves in steady flows.

The new state-of-the- knowledge, which was published in 2007 in the 2nd edition of the above mentioned monograph by Ben-Dor, will be presented in this review. Specifically, the hysteresis phenomenon in the $RR \leftrightarrow MR$ transition process, which until the early 1990s was believed not to exist, will be presented and described in detail, in a variety of experimental set-ups and geometries.

Analytical, experimental and numerical investigations of the various hysteresis processes will be presented.

References:

Ben-Dor G. *Shock Wave Reflection Phenomena*, Springer, New York, 1991.
Ben-Dor G. *Shock Wave Reflection Phenomena*, 2nd Ed., Springer, New York, 2007.

Single vesicle dynamics in various flows: Experiment versus theory

V Steinberg

Department of Physics of Complex Systems
Weizmann Institute of Science
Rehovot, Israel
Email: Victor.Steinberg@weizmann.ac.il

Dynamics of a single vesicle in shear, elongation, and general flows is investigated experimentally. Phase diagram of three vesicle dynamical states is obtained experimentally in both shear and general flows (Fig. 1). The new control parameter, the ratio of the vorticity to the strain rate ω/s, allows following an experimental path, which scans across the whole phase diagram with a single vesicle. Surprisingly, all three states and transitions between them are obtained on the same vesicle and at the same viscosity of inner and outer fluids. We reveal the physical nature of the key dynamical state, coined by us trembling (Fig. 2), which shows up in intrinsic shape instability on each cycle resulted in periodical bursting of higher order harmonics depending on the value of the control parameter proportional to ω/s. The dynamics of trembling state is compared with dynamics of a vesicle a time-dependent elongation flow, where the wrinkling instability was discovered, and similar features are identified. Quantitative comparison with recently proposed models and numerical simulations for vesicle dynamics is reviewed.

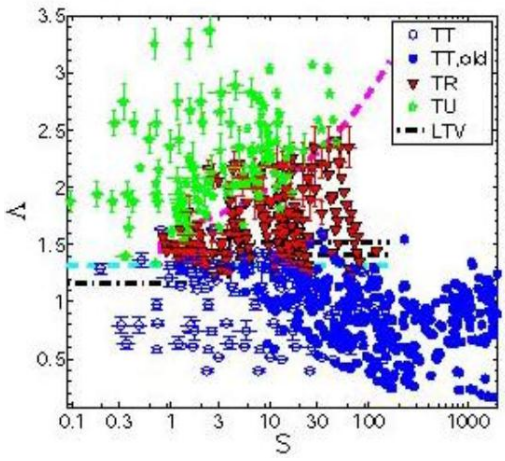

Fig. 1 Phase diagram of the vesicle dynamical states in a shear flow: tank-treading (TT) - blue circles, trembling (TR) - red triangles, tumbling (TU) - green stars

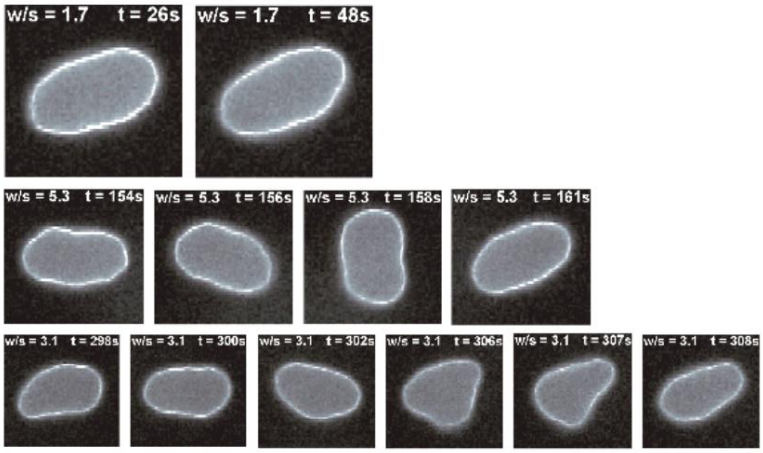

Fig. 2 Dynamical states of a vesicle: (a) TT; (b) TU; (c) TR

Keywords: vesicle dynamics, phase diagram, trembling motion

References:

J. Deschamps, V. Kantsler, V. Steinberg, Phys. Rev. Lett. 102, 118105 (2009).
J. Deschamps, V. Kantsler, E. Seghre, V. Steinberg, PNAS 106, 11444 (2009).
N. Zabusky, E. Segre, J. Deschamps, V. Kantsler, V. Steinberg, Phys. Rev. E., submitted (2010).

Granular Gases and Kinetic Theory

S. H. Noskowicz

School of Mechanical Engineering,
Faculty of Engineering,
Tel-Aviv University, Ramat-Aviv, Tel-Aviv 69978, Israel
Email: henri@eng.tau.ac.il

We present some of Professor Isaac Goldirsch's pioneering contributions to the understanding of granular gases. Granular matter can be defined as an aggregate of elementary macroscopic particles, grains, e.g., sand, powders, wheat, coal. Much of the wealth of behaviour of granular matter is due to the inelastic interactions between the grains. Granular matter appears in various states of matter depending on the density. At low to moderate density it is a gas or a fluid and the grains interact mainly by inelastic collisions. At higher density, in a compact state, it is a similar to a solid; the grain are in constant contact and experience mostly the effects of friction and contact elasticity and become partially or totally stuck (jammed).

In this talk we concentrate on the gas phase and the work done by Isaac Goldhirsch and collaborators (including the speaker) during the last decade. The field of granular gases has recently witnessed tremendous theoretical progress most of which is based on the application of the kinetic theory of gases, i.e. the Boltzmann equation properly modified to account for the inelastic nature of granular collisions. The Boltzmann equation applies only to dilute gases, i.e., gases in which the grain dimensions are far smaller than the mean free path and therefore colliding particles are only weakly correlated. When these collisions occur at a sufficiently rapid rate compared to the rate of change of the macroscopic fields, a hydrodynamic description of the gas can be obtained, and one can use the Boltzmann equation to produce constitutive relations. In early studies, constitutive relations, based on the Boltzmann equation, were derived only for the case of elastic collisions (e.g., Navier-Stokes equations). The application of kinetic theory to granular gases has proven capable of producing theoretical results which agree very well with physical and numerical experiments. Very dense granular (and elastic) fluids still pose serious theoretical challenges. The method of generating and supergenerating functions in kinetic theory invented at Tel-Aviv in Isaac Goldirsch's group has proved to be very powerful for solving the Boltzmann equation and will be shortly explained. The application to binary mixture will be described, as well.

Keywords: *Granular gas, Constitutive relations.*